AIAA JOURNAL
Vol. 45, No. 7, July 2007

Refinements in a New Adaptive Ordinal Approach to Continuous-Variable Probabilistic Optimization

Vicente J. Romero*
Sandia National Laboratories, Albuquerque, New Mexico 87185-0828
and
Chun-Hung Chen†
George Mason University, Fairfax, Virginia 22030

DOI: 10.2514/1.24892

A very general and robust approach to solving continuous-variable optimization problems involving uncertainty in the objective function is through the use of ordinal optimization. At each step in the optimization problem, improvement is based only on a *relative ranking* of the uncertainty effects on local design alternatives, rather than on precise quantification of the effects. One simply asks, "Is that alternative better or worse than this one?"not "*How much* better or worse is that alternative to this one?" The answer to the latter question requires precise characterization of the uncertainty, with the corresponding sampling/integration expense for precise resolution. However, in this paper, we demonstrate correct decision-making in a continuous-variable probabilistic optimization problem despite extreme vagueness in the statistical characterization of the design options. We present a new adaptive ordinal method for probabilistic optimization in which the tradeoff between computational expense and vagueness in the uncertainty characterization can be conveniently managed in various phases of the optimization problem to make cost-effective stepping decisions in the design space. Spatial correlation of uncertainty in the continuous-variable design space is exploited to dramatically increase method efficiency. Under many circumstances, the method appears to have favorable robustness and cost-scaling properties relative to other probabilistic optimization methods, and it uniquely has mechanisms for quantifying and controlling error likelihood in design-space stepping decisions. The method is asymptotically convergent to the true probabilistic optimum, and so could be useful as a reference standard against which the efficiency and robustness of other methods can be compared, analogous to the role that Monte Carlo simulation plays in uncertainty propagation.

I. Introduction

A VERY general and robust approach to solving optimization problems is via *ordinal optimization*, in which improvement at each step in the optimization problem is based only on a *relative ranking* of response, rather than on precise quantification of response. It is much less difficult and expensive to determine whether one response is greater/less than another, than to accurately quantify their response values ("...think of holding two objects to determine which one weighs more, versus trying to estimate their actual weights [by holding them]..." [1]); much more complex and accurate machinery is required to get accurate weights. Correspondingly, the ordinal approach appears to be naturally suitable for optimization problems involving nonprobabilistic and semiquantitative descriptions of uncertainty. In fact, it can be seen as a formalism of the ordinal-selection process employed by decision-makers in the real world when they deliberate over competing options for which the outcomes are highly uncertain.

For continuous-variable (C-V) design problems (continuously variable design options), non-gradient-based local optimizers such as simplex and pattern-search methods [2,3] and global methods such as genetic algorithms and DIRECT [4] can be used to search the design space, using ordinal comparison to select improvement steps. This paper considers C-V problems of optimization under uncertainty (OUU), in which ordinal comparisons are made of alternatives in the design space that have probabilistic information regarding their uncertainty.

C-V OUU problems are principally different from *stochastic optimization problems*, in which random stochastic noise in the objective function is a primary feature of the deterministic or OUU optimization problem. Specialized optimization techniques exist for this type of random stochastic uncertainty in the objective function [5]. In C-V OUU problems, the uncertainty in the objective function comes principally from fundamental uncertainty about the response or behavior of the system being optimized.

Fundamental concepts of probabilistic ordinal optimization are presented in this paper. In particular, efficiencies gained from exploiting spatial correlation of uncertainty and sampling in the design space are demonstrated on a low-dimensional probabilistic optimization problem. More sophisticated implementational possibilities are discussed, along with the merits compared with nonordinal approaches to probabilistic optimization.

II. Engineering-Optimization Problem Motivating Probabilistic Ordinal Concepts

A. Deterministic Optimization Problem

The probabilistic optimization problem considered here is an outgrowth of a deterministic optimization problem [6] in which heating conditions were sought that put a candidate weapon subsystem design most at risk. As shown in Fig. 1, the design problem is parameterized in terms of two key heating variables: 1) the radius r of a circular region of impinging fire on the top of the safing subsystem and 2) a coordinate x that moves the center of the "blow torch" on the device's surface along the cut-plane shown. A 3-D finite element conduction/radiation thermal model (described in [6]) is used to calculate the transient temperature response of the device. Figure 1 shows the calculated temperature of the device (cut

Presented as Paper 1826 at the 1st AIAA Non-Deterministic Approaches Conference, Newport, RI, 1–4 May 2006; received 8 May 2006; revision received 29 November 2006; accepted for publication 18 January 2007.

* Technical Staff Member, Model Validation and Uncertainty Quantification Department, P.O. Box 5800; vjromer@sandia.gov. Senior Member AIAA (Corresponding Author).

† Associate Professor, Department of Systems Engineering & Operations Research, 4400 University Drive, Mail Stop 4A6.

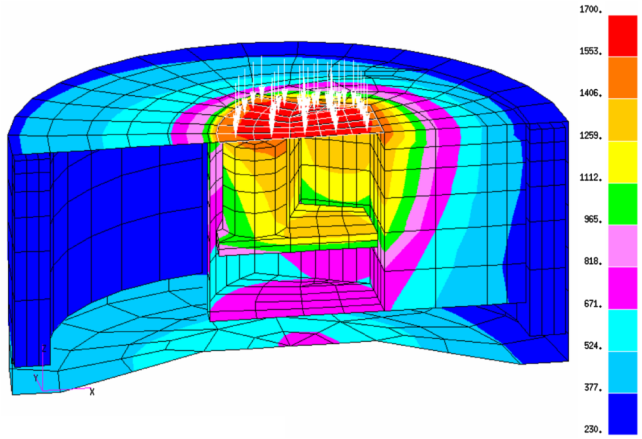

Fig. 1 Safing device exposed to circular region of heating.

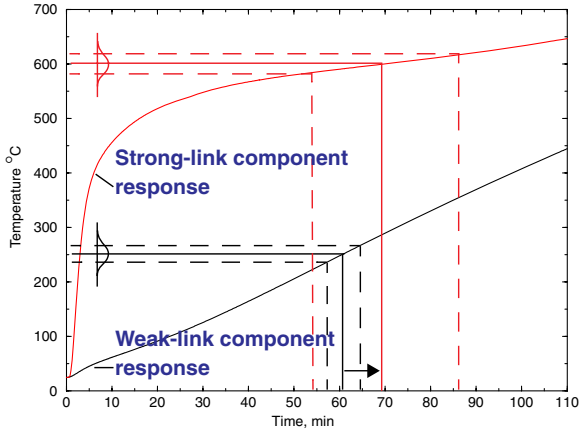

Fig. 2 Mean realization of each component's failure temperature (solid line) reflects through component temperature response curve into a failure time. The difference in component failure times, $t_{\text{fail}_{\text{SL}}} - t_{\text{fail}_{\text{WL}}}$, is the corresponding safety margin, shown by the right-pointing arrow for the positive margin here.

along its plane of symmetry) at some point in time for a particular radius r and location x of heating.

Figure 2 shows temperature histories for two safety-critical components within the safing device: a strong link and a weak link. The components are termed as such because the weak link must be thermally weaker and fail at a lower temperature than the thermally stronger strong link, to prevent inadvertent operation of the weapon.

Focusing just on the depicted *nominal* failure temperatures of the components (nominal $T_{\text{fail}_{\text{WL}}} = 250°\text{C}$ and nominal $T_{\text{fail}_{\text{SL}}} = 600°\text{C}$), an associated safety margin of time can be defined:

$$S = t_{\text{fail}_{\text{SL}}} - t_{\text{fail}_{\text{WL}}} \tag{1}$$

where the subscripts SL and WL denote the strong link and weak link. Here, $t_{\text{fail}_{\text{SL}}}$ and $t_{\text{fail}_{\text{WL}}}$ are the elapsed times (from time zero at the beginning of the thermal simulation) required for the links to reach their nominal failure temperatures. In Fig. 2, the safety margin associated with the nominal failure temperatures of the components is positive and has a value of about $S = +9$ min (right-pointing arrow in the figure). A negative or zero safety margin indicates that the strong link is not failing after the weak link, as desired, and the safing device is experiencing a vulnerability for that set of heating conditions and component failure temperatures.

The safety margin is a deterministic indicator of the safety of the device. A probabilistic indicator of the safety of the device will later be defined that takes into account the depicted uncertainty in the component failure temperatures.

In the optimization problem, the intent is to find the heating conditions that minimize the indicated safety of the device. This minimum corresponds to the heating conditions that most threaten the intended function of the safing device. If the vulnerability is deemed unacceptable, the design can be modified to sufficiently harden the device to these worst-case heating conditions.

In the *deterministic* optimization problem, the optimal values of the variables r and x are sought that minimize the safety margin of the device. As the $\{r, x\}$ variables are changed, the strong-link and weak-link temperature responses change and the value of the safety margin changes accordingly (assuming fixed nominal failure temperatures for the components). Thus, the deterministic safety-margin objective function $S(r, x)$ is navigated (minimized) in the deterministic optimization problem.

The deterministic optimization problem is complicated by numerical noise resulting from discrete time and space representation in the model [6,7]. On a more global scale, the deterministic optimization problem contains mathematical difficulties associated with navigating to a global minimum at $\{\text{r}, \text{x}\} = \{1.62, 0.782\}$ on a nonconvex design surface having a fold and several local minima, as described in [6,7].

Toward solving the deterministic local optimization problem, Newton-based nonlinear programming (NLP) methods [sequential quadratic programming, Broyden–Fletcher–Goldfarb–Shanno (BFGS) quasi-Newton, and quasi-Newton] from several different research and commercial optimization packages were tried with little success, as explained in [7]. Nonconvexity and noise resulted, respectively, in ill-conditioning and inaccuracy of the Hessian matrix of finite-differenced second-order derivatives.

To avoid these problems with the second-order information, first-order NLP conjugate-gradient methods were employed in [7] with more success, but still exhibited some noise-induced nonrobustness. The choice of finite difference step size for computation of sufficiently accurate gradients proved to be important. The initial starting point also proved to be important because of the noise.

The relatively high degree of model-discretization resolution required for sufficiently smooth computed response for reliable gradient-based navigation of the design space added large cost compared with the more noise-tolerant derivative-free optimization approaches applied in [8]. There, a simple coordinate-pattern-search (CPS) method was shown to be successful, with lower model resolution/cost requirements than the conjugate-gradient method. The CPS method was both more robust and less costly than the conjugate-gradient method.

More recently, a global-to-local optimizer devised with moving low-order polynomial local response surfaces to be efficient in the presence of small-scale noise was applied to this problem in [9]. The method performed considerably better than all those previously tried, in terms of the number of function evaluations required, cost of function evaluations (model discretization level required for accuracy), and robustness to noise level. The method was later recognized to be a type of surrogate-based *trust-region* optimization approach. Successful approaches in this vein had already been introduced elsewhere [10,11]. The general advantages of surrogate-based trust-region approaches for handling noisy optimization problems are now well recognized.

B. Probabilistic Optimization Problem

The associated probabilistic optimization problem is now considered. Figure 2 indicates that strong-link and weak-link failure temperatures trace out to relatively flat portions of the temperature response curves. This is truer for the strong link than for the weak link, but regardless, it can be seen that the component failure times are very sensitive to the failure-temperature values. Thus, moderate uncertainties in the component failure temperatures $T_{\text{fail}_{\text{WL}}}$ and $T_{\text{fail}_{\text{SL}}}$ can have a substantial impact on the uncertainty of the safety margin. In fact, when reasonable uncertainty bands 5% above and below the nominal failure temperatures are considered in Fig. 2, the corresponding bands in failure times indicate that the safety margin could vary from about 28 min at best to about -11 min at worst.

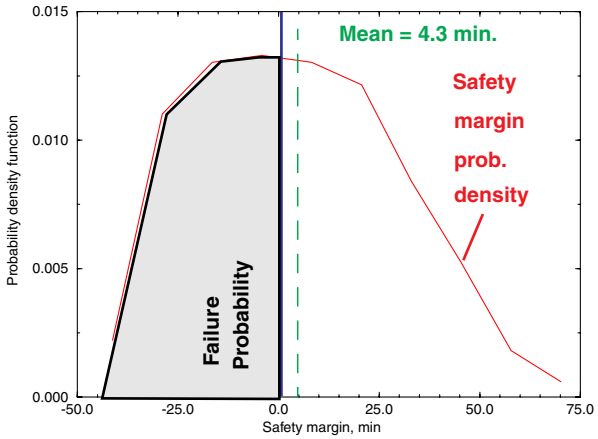

Fig. 3 Safety-margin probability density function at a particular set $\{r, x\}$ of heating conditions for uncertain strong-link and weak-link failure temperatures.

Thus, it is apparent that the effects of uncertainty in the component failure thresholds are very important in this problem.

1. Safety-Margin Distribution Due to Uncertain Component Failure Thresholds

For the purposes here, the strong-link and weak-link failure temperatures $T_{\text{fail}_{\text{SL}}}$ and $T_{\text{fail}_{\text{WL}}}$ are each assumed to be described by truncated normal distributions with means μ equal to the respective nominal failure temperatures of 600 and 250°C, and standard deviations σ equal to 3% of the means, or 18 and 7.5°C, respectively. (The distributions are truncated at 3σ above and below their mean values and then renormalized to integrate to unity.)

Multiple sets of weak-link and strong-link failure temperatures can be generated by standard Monte Carlo sampling, and then a safety margin can be computed for each set by using the time histories of the weak and strong links obtained from the thermal model run at the $\{r, x\}$ heating conditions. The resulting population of safety-margin realizations will be distributed with some probability density, as exemplified in Fig. 3. Associated statistics such as the mean, the standard deviation, and the probability of attaining a zero or negative safety margin can be calculated. For example, the mean safety margin denoted in the figure is +4.3 min for temperature-response curves obtained by running the model at the deterministically worst-case set of heating conditions $\{r, x\}_{\text{opt-det}} = \{1.62, 0.782\}$.

The deterministic safety margin for this set of heating conditions (and nominal failure temperatures of $T_{\text{fail}_{\text{WL}}} = 250$°C and $T_{\text{fail}_{\text{SL}}} = 600$°C) is about 2.5 min, or 40% less than the 4.3-min mean. This problem is clearly nonlinear in the uncertain parameters $T_{\text{fail}_{\text{WL}}}$ and $T_{\text{fail}_{\text{SL}}}$; otherwise, the mean safety margin would equal the deterministic safety margin at the mean values of the uncertain parameters. This nonlinearity may result in different optimal (worst-case) heating conditions $\{r, x\}_{\text{opt}}$ if component failure uncertainty is taken into account (rather than being ignored, as in the deterministic optimization problem).

Figure 4 shows a 3×3 grid of points over a small subset of the design space, centered about the deterministic optima $\{r, x\}_{\text{opt-det}} = \{1.62, 0.782\}$. Figure 5 shows magnitude bars for failure probabilities calculated at the nine points of the grid by Monte Carlo sampling over the strong-link and weak-link failure-temperature uncertainties. Thus, safety-margin distributions and corresponding failure-probability magnitudes (as in Fig. 3) are obtained at each design point. The optimization problem now is to *maximize* the *probabilistic* objective function for failure probability to determine the worst-case heating values of r and x.

2. Motivation for Probabilistic Ordinal Optimization in this Problem

The biquadratic response surface shown in Fig. 5 can be seen to not go exactly through the end points of the probability bars, because the

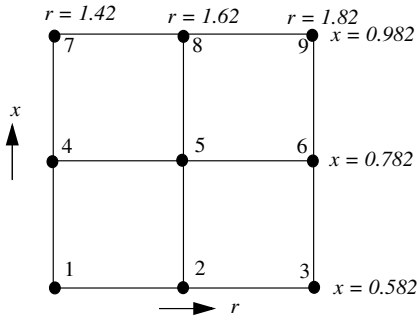

Fig. 4 Nine-point grid over an important subset of 2-D optimization space, centered at the point where the deterministic optimum for worst-case heating occurs.

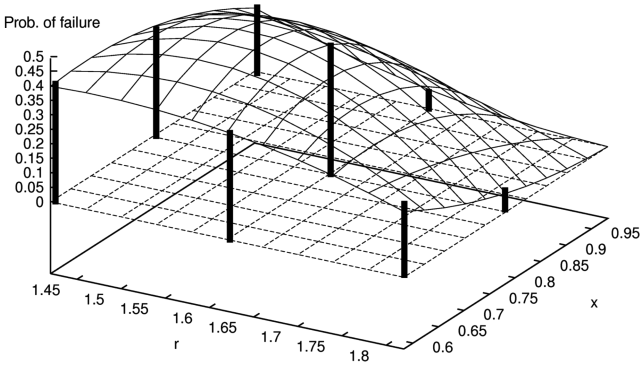

Fig. 5 Probabilistic objective function (biquadratic response surface built from Monte Carlo point estimates of failure probabilities at the nine grid points).

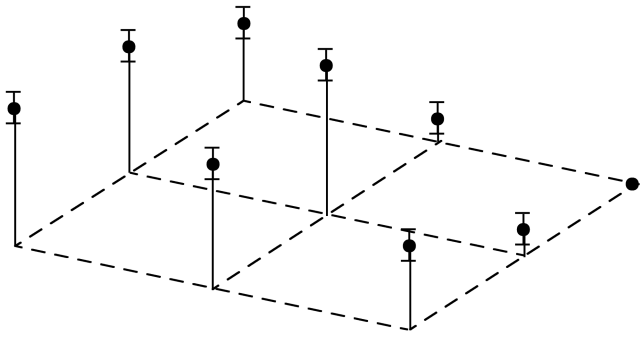

Fig. 6 Monte Carlo point estimates of failure probabilities with associated confidence intervals.

response surface was created from probabilities obtained from 500 Monte Carlo samples, rather than from the 1000 samples from which the bars are based. The mismatch between bar height and response-surface height varies somewhat over the design space. The mismatch reflects the fact that Monte Carlo estimates from a given number of samples have confidence intervals, as depicted in Fig. 6, that reflect uncertainty (potential error) in the point estimates.

The following questions then arise: What effect does the number of Monte Carlo samples have on the accuracy with which a probabilistic optimum can be identified in the design space? If one wants to identify the heating variables $\{r, x\}$ that correspond to the highest probability of device failure, how can the impact of Monte Carlo sampling errors be controlled? How many samples need to be taken at each point in the design space to shrink the confidence intervals small enough so that it is unambiguous as to which design point corresponds to the highest failure probability?

III. Fundamental Concepts of Probabilistic Ordinal Optimization

In addressing the preceding questions, it is noted that probabilistic ordinal optimization has been studied for some time in the operations research field (e.g., [12]), to compare discrete design alternatives (as opposed to continuous-variable design alternatives such as in this paper). In particular, the work has addressed apportioning Monte Carlo sampling amongst multiple uncertain or stochastic discrete systems, to most efficiently resolve their statistical behavior for the purpose of selecting the best option or several best options. The concepts and procedures apply whether it is desired to: 1) minimize the total number of samples required to reach a desired *probability of correct selection* (P{CS}) of the best option or several best options or 2) maximize the probability of correct selection for a given budget of total samples N_T, to be optimally apportioned among the various alternatives. In either case, the odds that the current identification of the best alternative(s) is correct can be estimated at every stage of the sampling.

The concepts of probabilistic ordinal optimization can also be applied to continuous-variable probabilistic optimization problems. For such problems, improvement steps in the design space can be taken based on ordinal ranking of candidate alternatives according to relative merit, rather than by attempting to resolve the actual merit value of each alternative as is done in nonordinal approaches (see [13,14] for brief overviews of some nonordinal approaches to OUU, such as surrogate-based and reliability-based methods). The relaxed ranking conditions for progress in ordinal optimization allow it to be more efficient than nonordinal methods for certain problems, as demonstrated in [15]. These latter approaches can introduce sources of noise and approximation error into the probabilistic objective function that can be avoided with probabilistic ordinal approaches (see for a discussion). Furthermore, for continuous-variable problems, the efficiency of sampling operations for ordinal ranking can be greatly increased by considering local spatial correlation in the design space, as explored in Sec. III.B. Additionally, advanced continuous-variable ordinal optimizers can be used, such as genetic algorithms, evolutionary simplex and pattern-search methods [2,3], and the simultaneous global/local search method DIRECT [4].

A. Independent (Uncorrelated) Designs

Consider two different designs or processes that each have some variability in their behavior or outputs. To compare the relative merit of the two designs, statistics of their relative merit can be compared. Thus, one can ask whether design A or design B has the higher mean output, or the lower probability of meeting or not meeting some acceptable threshold of behavior, or the smallest variance in the product produced.

The behavior or output of these independent designs can be sampled to generate statistics of their tendencies. For mean and probability, it is known from classical confidence interval theory that the values $\hat{S}_A$ and $\hat{S}_B$ of a statistic calculated from finite sampling will be realizations from normal distributions with means S_A and S_B, the true means. The normal distributions have variances $\sigma^2_{\hat{S}_A}$ and $\sigma^2_{\hat{S}_B}$ that decrease as the number of samples increases. Figure 7 depicts normal distributions of the calculated statistics from the two designs being compared.

Under limited sampling, the two normal distributions each have nonzero variance, which means that the distributions overlap to some degree, as illustrated in Fig. 7. Hence, it is possible for a calculated statistic $\hat{S}_A$ of design A to have a value greater than the calculated statistic $\hat{S}_B$ of design B, even though this is not the case for the true values S_A and S_B. If the optimization goal is to pick the design that maximizes the critical statistic (maximizes the mean output rate or probability of acceptance), then there is a nonzero probability that a misleading indication would be given that design A is better than design B. The more the error distributions overlap, the less certain it is that the chosen design is indeed the better design.

As the number of Monte Carlo samples of each design increases, the critical statistics become better resolved. That is, their confidence

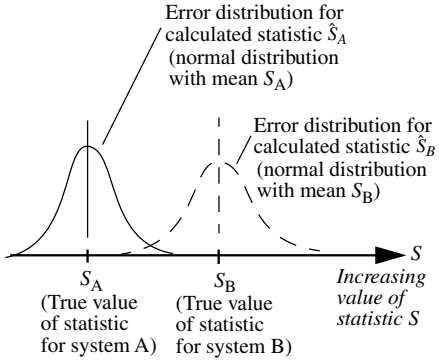

Fig. 7 Normally distributed errors in Monte Carlo estimates of statistical behaviors of two different systems.

intervals decrease such that it becomes increasingly apparent which alternative has the better statistical behavior. Hence, the probability of making a correct selection between the two alternatives (i.e., the P{CS}) increases with more Monte Carlo sampling.

The P{CS} value has the property of converging to 100% at an exponentially fast rate as the number of samples increases [17]. This is a much faster rate than for resolving the individual alternatives' behavioral statistics. That is, the standard deviations of the individual distributions in Fig. 7 only decrease at a rate of the inverse square root of the number of samples of that alternative. However, by looking at the figure, it is intuitive that as the "width" (standard deviation) of either or both probability density functions decrease at a fixed rate, the question of which alternative's value is greater is resolved at a much faster rate. In fact, such differentiation occurs at an exponential rate with the total number of samples expended, N_T, whether only one alternative is sampled or both are sampled: $\text{P\{CS\}} \geq 1 - \alpha e^{-\beta N_T}$ [17].

Reference [16] describes a methodology for calculating the probability of correct selection when only two design options are considered at a time. A requirement can then be posed to determine to a given level of statistical assurance P{CS} that the option picked has the better actual figure of merit. Meeting this requirement necessitates sampling the alternatives' behaviors a sufficient number of times. The question then arises: What is an adequate number of samples?

A unique answer to this question does not exist. Figure 7 shows that a desired overlap (or nonoverlap, as the present requirement is stated) may be attainable by increased Monte Carlo sampling to manipulate the spread (variance) of alternative A's distribution, of alternative B's distribution, or some combination of both (only this last case is guaranteed to always work). If a combination of both is used, there is not a unique combination that will attain the desired result.

The way to approach the sufficiency issue is to then ask a second question: What is the most *efficient* way to achieve sampling sufficiency for a given P{CS} requirement? This question *does* have a unique answer, and this answer minimizes the total number of samples N_T apportioned between the two alternatives that will achieve the desired P{CS} level. In comparing two alternatives, the optimal apportionment of samples amongst the two alternatives is relatively easy to obtain, as described in [16]. In comparing more than two alternatives, the optimal solution from [18], referred to as the *optimal computing budget allocation* (OCBA), is much more involved and difficult to obtain. Furthermore, calculation of P{CS} itself is much more difficult than the well-known approach for two alternatives.

Though the possibilities of increasing the efficiency are myriad, a simple implementation of probabilistic ordinal optimization (comparing only two alternatives at a time) was applied in [16] to the probabilistic optimization problem defined earlier. A requirement of 95% P{CS} was imposed in the ordinal comparisons, and a simple CPS algorithm [2] was used to systematically progress toward the optimum in the continuous 2-D *r-x* design space. At the end of the process, a high confidence existed that the probabilistic optimum

obtained was the true optimum among the designs considered. A more sophisticated application considering multiple alternatives simultaneously on our test problem is demonstrated in this paper in Sec. IV.C. In comparing more than two alternatives, a simultaneous comparison approach is often more efficient than the sequential pairwise method of comparing two at a time and then dropping the "loser" and comparing the "winner" to the next alternative in the list, until all alternatives have been considered. If one of the alternatives happens to be much better than the current best point and all the other alternatives in the comparison, then simultaneous comparison will generally be more efficient than sequential pairwise comparison. The sequential pairwise method has its own appeal, however, because of its relative simplicity of implementation.

To the authors' knowledge, no other methods for probabilistic optimization currently offer a quantitative assessment of correctness probability. If fact, the combination of CPS optimizer with probabilistic ordinal optimization as discussed here (with either pairwise or simultaneous comparisons) is asymptotically convergent to the true local probabilistic optimum [16]. Thus, probabilistic ordinal optimization may be usable to provide a reference standard against which the accuracy and efficiency of other OUU methods can be compared, analogous to the role that Monte Carlo simulation plays in uncertainty propagation.

B. Correlated Designs: Efficiency from Spatial Correlation of Uncertainty in Continuous Design Spaces

The full-variance distributions of Fig. 7 apply for completely uncorrelated designs, as is often the case when comparing discrete alternatives in the realm of operations research. For continuous design spaces, however, closely neighboring points in the design space can have closely correlated uncertainties. The efficiency-enhancing prospects of spatial correlation of uncertainty in the design space are investigated here.

Figure 8 illustrates the correlation issue. The mapping of uncertainty distributions at two neighboring design points is shown. For convenience of illustration, the uncertainties in this particular figure derive from stochastic noise in the tolerances that can be held in the design variable. This uncertainty (as a function of location in the design space) maps through the deterministic input/output function of system behavior, as shown. Resulting output response uncertainties are depicted on the vertical axis. Though shown on the design-variable axis, uncertainties in other (non-design-variable) inputs to the system may exist. These uncertainties would similarly map into response uncertainties. Thus, in general, the response distributions may have contributions of uncertainty from design variables and/or other system variables.

In any case, as the compared points in the design space get closer, the inputs to the system or design look more alike. Furthermore, the response function that maps inputs in the design and uncertainty spaces to points on the response axis becomes more alike. This means that if Monte Carlo realizations of the involved uncertainties are taken with the exact same random-number-generator starting seed at each design point (termed *spatially correlated sampling* in [15]), the uncertainty realizations and the response realizations will be very strongly correlated, as illustrated in Fig. 8 for the *i*th sample taken at each design point. That is, on the design-variable axis, uncertainty realizations at the neighboring design points will come at similar percentile locations in the input uncertainty distributions. Likewise, the mapped response values for these input uncertainty realizations will occur at similar percentiles of the response distributions. Thus, the input/response realizations are spatially correlated (at least locally) in the design space.

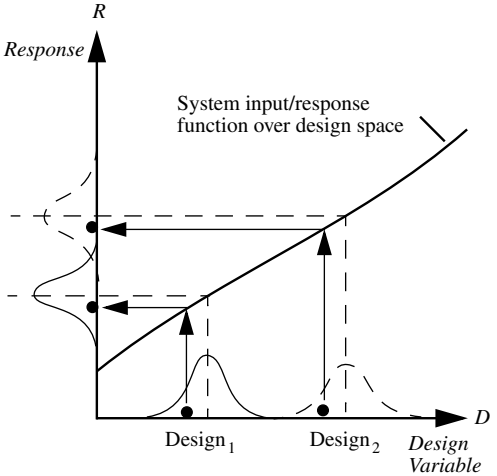

Fig. 8 Correlated sampling of input/response distributions at two different points in design space.

1. *Spatial-Correlation Deterministic Efficiency Limit*

In the spatial-correlation deterministic efficiency limit, the input uncertainties and the system response function that maps the input uncertainties to response uncertainty do not change over the design space. Therefore, the response uncertainty distribution does not change over the design space, except for relative position on the response axis. Hence, it is trivial to identify which design point has the highest mean response or probability of response exceeding some threshold value. Only one correlated Monte Carlo sample of the uncertainty at each design point is needed to locate the relative position of the response distributions. If the single sample at each design point is evaluated at the nominal (midrange) values of the input uncertainties, then this is a balanced deterministic transform of the probabilistic optimization problem. Note that with a single sample, it cannot be said what the mean or probability value is at each design point, but only which design point spawns the highest or lowest such value. This is sufficient to select the best move for optimizing the probabilistic objective function.

Thus, the conditions just described enable probabilistic OUU problems to be treated as deterministic optimization problems, with the attendant simplification and cost savings that this brings. This limiting case, in which perfect spatial correlation in continuous-variable probabilistic optimization problems causes them to be degenerate such that they can be recognized and treated as deterministic optimization problems, is termed the *spatial correlation efficiency limit* [15]. An ordinal perspective identifies (and exploits) this determinism, whereas other OUU approaches may not. Indeed, the authors have seen several instances in the literature in which problems of this nature have been expensively solved as probabilistic optimization problems instead of deterministic optimization problems.

2. *Efficiency from Uncertainty Variation Dominated by Nominal Response Trend in Design Space*

The spatial-correlation deterministic efficiency limit just described features a mechanism that allows degenerate probabilistic OUU problems to be treated as deterministic optimization problems, with the attendant cost savings. Because there is no response-uncertainty variation in the design space, the OUU problem is fully degenerate. This is a limiting case of a more general circumstance in which response-uncertainty variation in the design space is substantially dominated by the nominal response variation, such that effective progress in the probabilistic optimization problem can be made by solving a deterministic nominal representation of the OUU problem. Such dominance frequently exists in probabilistic optimization problems, particularly at stages of global and early local search. This allows successful initial treatment as a deterministic optimization problem that enables relatively inexpensive location of an initial point in the design space (deterministic optimum) that is relatively close to the probabilistic optimum. From this starting point, OUU methods are applied to find the probabilistic optimum.

Figure 9 illustrates the issues. The middle histogram in the figure corresponds to the safety margin uncertainty distribution (Fig. 3) at the nominal deterministic optima $\{r, x\}_{\text{opt-det}} = \{1.62, 0.782\}$. The histograms on either side correspond to the neighboring points 4 and

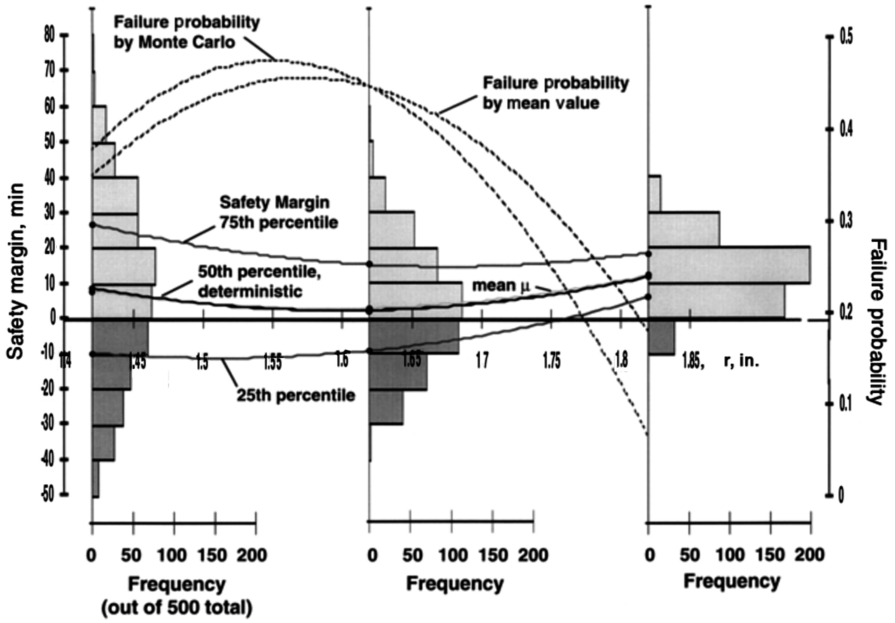

Fig. 9 Histograms of response (safety margin) distributions at three points (4, 5, and 6 of the nine-point grid in Fig. 4) along an $x = 0.782$ cut of the optimum region of the design space.

6 of the nine-point grid of Fig. 4. In Fig. 9, the nominal deterministic response is approximated by a quadratic curve through the 50th percentile locations on the safety-margin distributions. The location of the probabilistic optimum relative to the deterministic optimum is controlled by the local trends in the uncertainty behavior. In the present problem, the mean trend of response (as indicated by the 50th percentile curve in Fig. 9) rises to the left of the deterministic minimum. As the mean trend of response rises, the variance of the safety-margin distribution has to increase commensurately for the amount of the distribution beneath the $S = 0$ axis to keep increasing. At some point, even though the response variance keeps increasing in this direction, the effect of the rising mean trend of behavior overwhelms the effect of the increasing variance, and the failure probability begins to decline. This is reflected in Fig. 9 by the failure probability curves' maxima to the left of the deterministic optimum. These curves are quadratic fits to failure probabilities at grid points 4, 5, and 6, calculated by 1) 500 Latin-hypercube Monte Carlo samples and 2) a five-sample, central-difference, first-order second-moment (FOSM) method (e.g., see [19]).

Because the deterministic objective function is flat (has no gradient) at the deterministic optimum point 5, further progress in the probabilistic optimization problem can only be made according to the nonzero uncertainty gradient there, as explained next. Consequently, the deterministic approach to the probabilistic optimization problem must be abandoned in favor of a true (nondegenerate) probabilistic optimization approach that is driven by the uncertainty gradient.

At the deterministic optimum point 5 in Fig. 9, an obvious uncertainty gradient exists. That is, the safety-margin variance changes meaningfully as the r coordinate is traversed leftward from the minimum point 5 of the deterministic objective function; the histograms of response and their associated 25th, 50th, and 75th percentile curves increasingly spread out, signifying increasing response variance in this direction. Because the deterministic trend curve is flat at the deterministic optimum, any nonzero uncertainty gradient there will push the probabilistic optimum off of the deterministic optimum. The direction in which the variance of the safety margin increases is the direction in which more of the distribution will fall below the $S = 0$ threshold (horizontal axis in Fig. 9), at least initially, as the r coordinate is varied from the deterministic optimum. This is therefore the direction in which the failure probability will increase (at least initially) and the direction in which the probabilistic optimum (maximum failure probability) will lie. Hence, if sufficiently accurate techniques are available to determine the direction of the uncertainty gradient, or if suitable ordinal optimization is used as discussed in the next subsection, then one can proceed from the local deterministic optimum to the local probabilistic optimum.

More generally, beyond the optimization problem here, in a multimodal probabilistic optimization problem, the global optimum may not be reachable from the global deterministic optimum using *local* OUU methods (which are the subject of this paper). Nonetheless, if the uncertainty gradient is zero at a deterministic optimum, then the location of the deterministic optimum is at least a local optimum of the global probabilistic optimization problem, as there is no uncertainty gradient to push the probabilistic optimum off of the deterministic optimum. When the uncertainty gradient is zero over the entire design space, the location of the deterministic global optimum is also the location of the global probabilistic optimum. In this case, the probabilistic optimization problem can be treated as a deterministic optimization problem, as was explained in the previous subsection associated with the spatial-correlation efficiency limit.

Another case can be imagined in which the uncertain inputs to the system, and/or the system behavior function that maps the inputs to response uncertainty, change over the design space but the resulting response distribution does not. Here, too, the global deterministic and probabilistic optima occur at the same location in the design space. Even with correlated Monte Carlo sampling over the design space, the correspondence changes between sampled percentiles of the input uncertainties and their associated response percentiles. Thus, the response realizations at design points will become more weakly correlated in their percentiles of response as the distance between the design points increases. Hence, in contrast to the perfect-spatial-correlation special case, it is essential here that the single realization at each design point (in the deterministic analogue of the probabilistic optimization problem) occurs at the midrange values of the uncertain inputs. Then the spatial discorrelation of the resulting output realizations will be minimized, and the probabilistic optimization problem can be approximated as a deterministic optimization problem. Because this sampling strategy also works for the special case of perfectly correlated uncertainty in the design space, it is a good practice to always use the midrange uncertainty values in the deterministic transform of the probabilistic optimization problem.

If only one probabilistic optimum exists in the design space, then this global optimum can be reached from the deterministic optimum (as is the case for the optimization problem in this paper). Furthermore, for such unimodal probabilistic optimization prob-

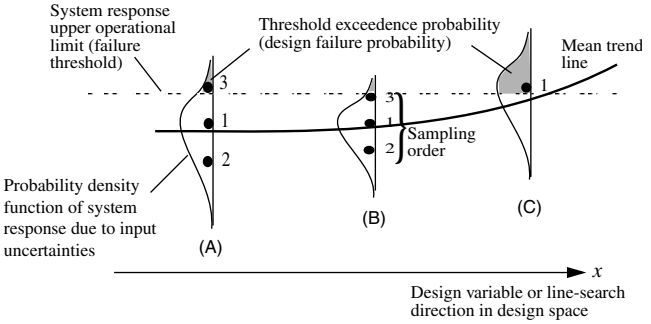

Fig. 10 Correlated sampling of response behavior of three design alternatives at points A, B, and C in the design space.

lems, if the uncertainty gradient is zero at the deterministic optimum, then this is also the location of the probabilistic optimum, because there is no uncertainty gradient to push the probabilistic optimum off of the deterministic optimum. In the extreme case in which the uncertainty gradient is zero everywhere over the design space, it is therefore also true that in the unimodal problem, the deterministic and probabilistic optima occupy the same location in the design space.

3. *Point-of-First-Separation Ordinal-Selection Efficiency Mechanism*

As was established in the previous subsections, deterministic-scale efficiency in the probabilistic optimization problem can be achieved when the influence of the uncertainty gradient is overwhelmed by mean behavioral trends. In this case, a single ordinal comparison will suffice for making effective optimization decisions in the probabilistic OUU problem. Conversely, when the effect of the uncertainty gradient dominates the effect of the underlying mean trend of behavior, as ordinarily occurs at the location of the deterministic optimum, it is necessary to turn from a deterministic treatment of the OUU problem to one in which more than one correlated sample per design point is necessary for successful progress in the problem.

The next level of sampling treatment that is suitable is coined the *point-of-first-separation* (PFS) ordinal-selection method. The PFS method can be thought of as an initial-stage implementation of the regular ordinal-optimization method. The PFS method truncates the sampling at the earliest possible ordinal-decision point, on the expectation that more sampling will only serve to confirm more strongly (and not overturn) the early indication of ordinal superiority of the best design. This expectation assumes that reasonably strong spatial correlation of the uncertainty will exist at the relatively small design-space scales involved in the final movement from the deterministic to the probabilistic optimum. (Recall that perfect or absolute spatial correlation of uncertainty occurs in continuous-variable problems as the distance between design points approaches zero.) A later demonstration on the OUU problem indicates that the PFS method is surprisingly efficient and effective.

The PFS method is explained with the help of Fig. 10. Three design alternatives (A, B, and C) are being compared in the figure to determine which has the lowest probability of failure. This illustration concerns failure-probability minimization rather than maximization, but the same principles apply whether seeking to maximize or minimize probability.

To start, a single correlated Monte Carlo sample of the response uncertainty of each design is evaluated. The sampled response of design C has a response value greater than the upper operating threshold level for acceptable system response. The first sample for the other two designs does not produce a threshold exceedence. On the assumption of closely spatially correlated sample realizations (i.e., the *n*th correlated Monte Carlo sample of each response distribution lies approximately at the same percentile on each distribution), this first sample already implies that design C will have a larger integrated failure probability than designs A and B. Because the objective is to identify the design with the lowest failure probability, design C can be immediately eliminated from further consideration.

A second correlated sample is then taken from the two designs still in contention. Neither of the remaining designs A and B indicates a failure (threshold exceedence) with this second sample. Of the two, design A has lower response values to this point and thus would appear to be the better candidate at this point. However, here is a case in which the influence of the uncertainty gradient is stronger than that of the underlying mean trend and dominates the determination of failure-probability magnitude. Hence, selection of the best alternative from indications so far would lead to an incorrect selection.

The least expensive strategy that can often be successful under dominant influence of the uncertainty gradient is to continue the correlated sampling of the remaining designs until one or several become distinguished from the rest by a difference in response status relative to the critical threshold in the problem. This occurs on the third correlated sample in Fig. 10. The response value of design A lies above the threshold, whereas that of design B lies below the threshold. On the assumption of spatially correlated percentile realizations, this third sample implies that similar percentiles of response for designs A and B, respectively, lie above and below the threshold. Therefore, it is implied that design B will have a lower integrated failure probability than design A.

In this contrived problem, it takes a total of seven Monte Carlo samples apportioned among the three initial candidate designs to

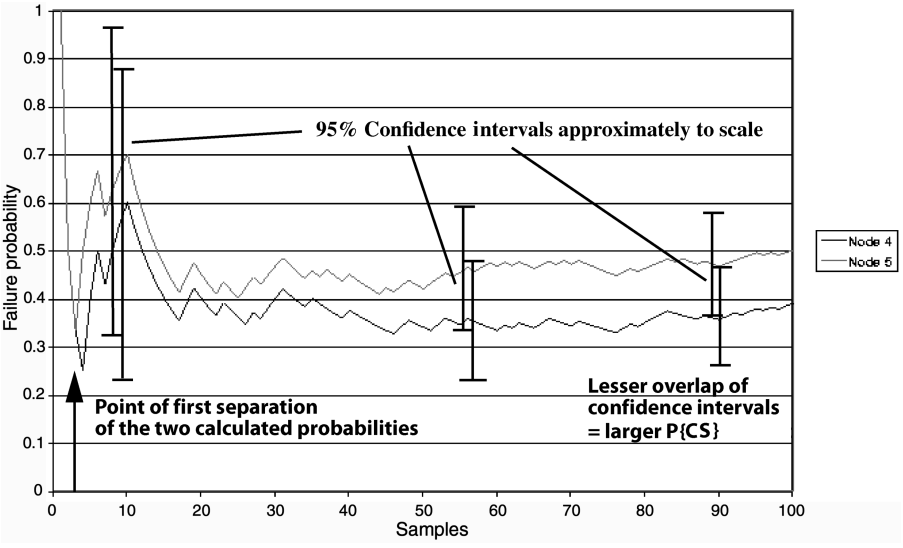

Fig. 11 Failure probabilities by correlated sampling of response behavior at design points 4 and 5 of the nine-point-grid subspace (Fig. 4).

identify the correct design. With a different sample placement and ordering that would accompany a different random-number-generator initial seed, a different total number of samples might be required. If, for instance, the sampling order in the figure was reversed, then with the first sample of each alternative (sample 3 in the figure), both designs A and C would be discarded immediately. Design B would be correctly selected at a total cost of only three samples. Therefore, the total number of samples employed in this truncated version of the full probabilistic ordinal selection process will vary, depending on the specific random-number-generator starting seed. This is also true for full probabilistic ordinal optimization.

Figure 11 shows some results of an empirical investigation of the PFS method. Calculated failure probabilities at points 4 and 5 of the nine-point grid (Fig. 4) are shown versus the number of correlated Monte Carlo samples of each design. With the fourth sample of each design, a separation in the calculated failure probabilities occurs. The separation wavers, but generally grows as the sampling increases. Once the separation occurs, the calculated probability values never cross each other, and so a correct ordinal selection was made just after the point of first separation. Any added sampling simply serves to decrease the confidence intervals about the calculated probability estimates, thereby increasing the probability, P{CS}, that the initial indicated separation is correct. The correlated sampling shown in Fig. 11 takes 202 samples total (101 each) to achieve a P{CS} of 95% under equal sampling of the two alternatives.

Because of the difficulty involved otherwise, all P{CS} values we state are calculated ignoring any spatial correlation of uncertainty in the design space. When such positive correlation exists, corresponding P{CS} values will be higher than when calculated on the basis of independent, uncorrelated designs [20]. Hence, the numerical values of P{CS} appearing in this paper may substantially understate the actual probabilities of correct selection.

Under optimally efficient (nonequal) OCBA sampling of the two alternatives, only 134 samples total are required to attain 95% P{CS} [16]. In contrast, the point of first tangible indication in Fig. 11 occurred after only eight samples (four of each alternative).

The noncrossing of probability curves (once initially separated) that is exhibited in Fig. 11 also occurs for all other two-alternative comparisons possible among the points of the nine-point grid. For any problem, it appears that the more local the comparisons (as when the probabilistic optimum is being converged to in the final stages of local optimization), the more similar the sampled response percentiles should be under correlated Monte Carlo sampling, and therefore the better the chance of correct selection by the point-of-first-separation mechanism.

PFS ordinal selection is used in [15] to successfully step to the probabilistic optimum of the present problem (Sec. II.B) with a simple CPS optimizer. The cost of solving the probabilistic optimization problem was 31 samples from the starting point. The same probabilistic optimum was found in [16], with 95% P{CS} at each CPS selection step. That result, having a very high probability of correctness, took 2721 samples to establish. Thus, PFS ordinal selection gave the same result but was tremendously cheaper. Note that the application problem here was not contrived in any way to be favorable to the PFS ordinal-selection method.

By comparison, the least expensive nonordinal approach possible for guiding the CPS search is to use a FOSM mean-value method [19] to estimate failure probability at the various candidate points in the CPS search. This would have required 30 samples for one-sided differencing and 50 samples for more robust central differencing. Thus, only in the best possible case [use of the lowest-cost probability-quantification method available (linear FOSM), yet also no significant error in the calculated failure probabilities] could an explicit probability-resolution approach be as inexpensive as the 31-sample PFS ordinal method at making correct stepping decisions in the test problem. This is a reasonable first indication of the relative efficiency of the PFS ordinal OUU approach. Reference [16] presents other reasons why this approach is expected to possess potential advantages over other OUU approaches in terms of robustness and cost-scaling as the number of design and/or uncertain variables increase in the OUU problem.

IV. Demonstration of a Combined Adaptive Probabilistic Ordinal OUU Method

An adaptive probabilistic ordinal OUU method is demonstrated in this section that combines the elements described in the previous subsections. The optimization goal in this example is to move in the design space to identify the optimal values of the fire-heating parameters r and x that maximize the probability of failure of the safing device.

A. Deterministic Initial Phase of the Method

The first element of the strategy is to employ a "preconditioner" to the probabilistic optimization problem by solving a representative deterministic version. This is done by temporarily fixing the uncertainties in the problem to their mean values and then solving the corresponding deterministic optimization problem. For the present problem, this was done with a variety of deterministic optimization approaches, as reported in Sec. II.A. The resulting deterministic optima, $\{r, x\}_{\text{opt-det}} = \{1.62, 0.782\}$, define the center (point 5) of the nine-point grid in Figs. 4–6.

B. Point-of-First-Separation (Economical Ordinal Selection Under Uncertainty) Phase of the Method

Starting from the deterministic solution, the probabilistic optimization is begun at a suitable initial probing scale in the design space, which may or may not be the same as the final probing scale in the deterministic precursor problem. The probing scale denoted by the nine-point grid is the initial probing scale to be used for this demonstration. A simple probing/stepping algorithm is used to

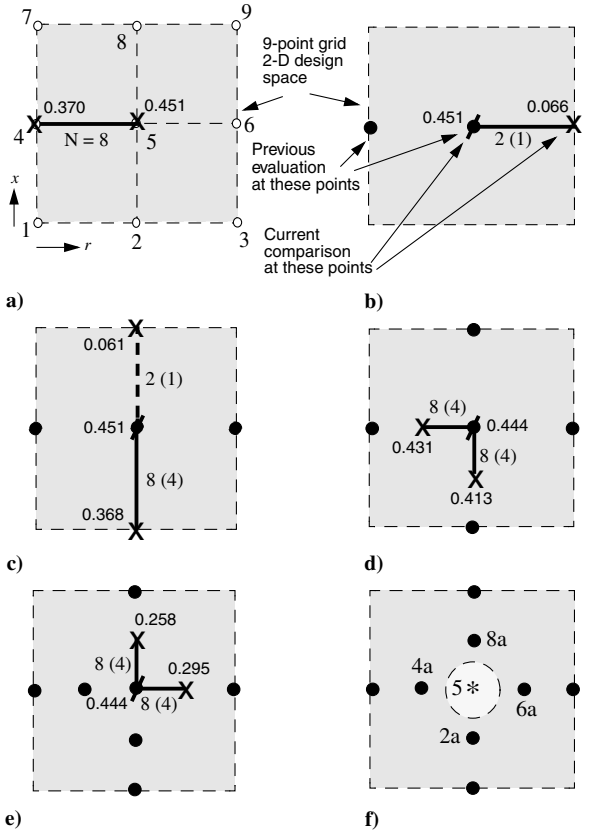

Fig. 12 Two-dimensional design optimization in the nine-point-grid design space by a simple space-searching algorithm and ordinal decision-making for better designs by pairwise PFS selection criterion based on closely related (correlated) uncertainty of nearby designs in the continuous-variable design space.

facilitate illustration of the concepts here. Much more sophisticated ordinal optimizers could be employed, as mentioned elsewhere in this paper.

When starting the OUU phase, the deterministic trends about the starting point 5 are known from the deterministic phase of the problem. The deterministic trend information is used for an initial indication of which direction appears most likely, based on the deterministic results, to yield the fiercest competitor to the current best point in the design space.

Here, the closest deterministic competitor to the final deterministic optimum lies at the left-center point 4 of the nine-point grid. Hence, the PFS correlated sampling method is applied to design points (alternatives) 5 and 4 in the design space. Recall that the PFS method samples both designs equally. This is done with correlated Monte Carlo sampling until the first signal of advantage of either design. The point of first separation occurs after just four samples of each alternative, as established in Fig. 11 and the previous subsection. Figure 12a depicts this comparison. The figure notes that $N = 8$ samples total (four for each alternative) are required for the comparison, that is, to get to the point of first indicated separation of probability values. For reference, the true failure probabilities of the alternatives being compared are printed in the figure.

With the center point having provisionally distinguished itself as having a higher failure probability than the grid point to its left, the next course of action is to determine whether the apparent trend of rightwardly increasing failure probability continues in going from grid point 5 to grid point 6. As shown in Fig. 12b, only two samples (one sample for each alternative) are necessary to provisionally signify that the center point has the higher probability of failure. It is to be expected that a very low number of samples would be necessary for this determination, given the large difference between the actual failure probabilities at the two points, as noted in the figure. The first safety-margin realization at point 6 is positive, or above the safety threshold, indicating an initial failure-probability estimate of zero. Conversely, the correlated first sample at the center point 5 is negative, or below the safety threshold, indicating an initial failure-probability estimate of one. Thus, the designs immediately separate in terms of their indicated safety after just one seed-correlated sample of each. Listed in Fig. 12b by the number 2 is the number 1 in parentheses. The number in parentheses is the number of new samples that must be drawn for the comparison. Only one new sample, of design 6, was needed here; the sample for the center design 5 was taken from its previous comparison against alternative 4.

Thus, for the current level of granularity (grid-probing scale) of the design space, the indicated maximum failure probability is at the center point 5 in the r design coordinate. We now consider the x design coordinate. The deterministic trend at point 5 has the nominal safety-margin objective function decreasing in the direction from point 5 to the bottom-center point 2 of the nine-point grid. Therefore, a PFS comparison is performed between design points 5 and 2. As noted in Fig. 12c, the failure probabilities at the two design points are relatively close. A total of eight samples (only four new, all at design point 2) are required to tangibly distinguish the center point 5 as having the higher failure probability. A consequent comparison of points 5 and 8, also depicted in Fig. 12c, again indicates that point 5 has the highest failure probability. This comes at a cost of only one new sample, of design 8.

Having exhausted all coordinate directions about the current best point at the current scale of resolution of the design space, a contraction is implemented to determine whether something off the center point at a smaller probing scale will possess an increased failure probability. Here, a new variant of the search procedure is used, just to demonstrate the possibilities.

The comparisons in Fig. 12d are driven by a desire to leverage off of the indicated directional trends of increasing failure probability in the negative r and x directions, as signified by the comparisons at the coarser probing scale. From considerations of the deterministic trends, the contracted alternative 4a to the left of center is compared first. Only eight samples (just four new ones, at point 4a) are required with PFS ordinal selection to dismiss design 4a, even though its failure probability is 0.431, whereas the center point 5 probability is a very close 0.444 (this is quite striking). Next, instead of comparing the rightward contracted point, as per the scheme of logic at the coarser probing scale, we take the option of first considering the most promising directional step in the other design variable. Only eight samples (just four new ones, at the downward contracted location 2a) are required with PFS to dismiss design 2a, even though its failure probability of 0.413 is relatively close to design 5's probability. Note that with this comparison scheme, designs 5, 2a, and 4a could be simultaneously sampled and compared under the PFS methodology. If one of the alternatives happens to be much better than the current best point and (all) the other alternative(s) in the comparison, then simultaneous comparison will generally be more efficient than the sequential-pairwise-comparison approach used here.

Having not found a better candidate among the initially indicated most promising designs 2a and 4a, candidate designs at opposite perturbations from the current best point 5 are evaluated next to see if the upward trends of failure probability continue in the rightward and upward directions (as established by the initial comparisons of designs 4a and 2a, respectively, to point 5). Hence, the next two candidates to be tested are designs 6a and 8a, at the rightward and upward contracted locations shown in Fig. 12e. Only eight new samples (four of each new candidates 6a and 8a) are required to provisionally dismiss these candidates as having lower failure probability than the reigning best design at point 5.

At this juncture, contraction can be implemented again and the optimization process can be continued, or the process can be suspended for fiscal or physical reasons (i.e., when the probing step size becomes less than the level of resolution uncertainty within which it is desired to resolve the optimal values of the design variables r and x). For the purposes of this demonstration, we elect to end this PFS phase of the optimization procedure and get on to the next phase. Figure 12f conveys that in stopping here, the center point is provisionally deemed to have the highest failure probability in the space, within the resolution uncertainty indicated by the lightly shaded region about the identified optimal point (asterisk) in the design space.

An *approximate* P{CS} (APCS) can be calculated to assess the confidence that design 5 is truly the best among the five finalists 2a, 4a, 6a, 8a, and 5. The *expected value* of APCS is P{CS}, which converges to a probability of one as the number of samples increases [18]. The current realization of APCS, based on just four samples of each design's probabilistic behavior from the PFS procedure, is 0.18. This value is based on just 20 samples among the five candidate designs and so is very tentative. Even if the relatively low APCS value of 0.18 is considered acceptable for the present purposes, we will next see that APCS estimates (particular realizations) can be exceedingly unreliable at low levels of samples. Therefore, we do not put much faith in this estimate. However, this does not mean that we strongly doubt that PFS identified the best design, just that we doubt the associated value of APCS calculated with so few samples. For more concrete assurance that the PFS selection is indeed the correct one, the OCBA process can be pursued, as demonstrated next.

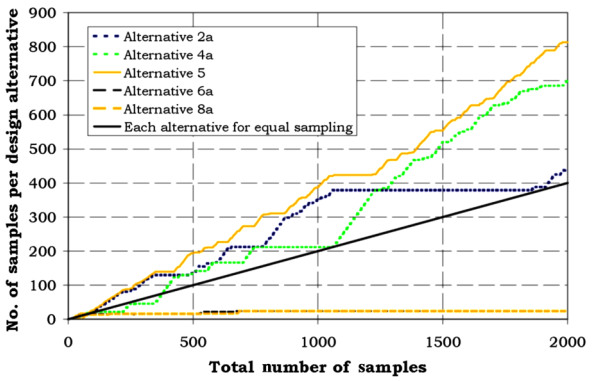

Fig. 13 OCBA apportionment of samples to candidate design finalists. In the end, the most samples go to the best designs.

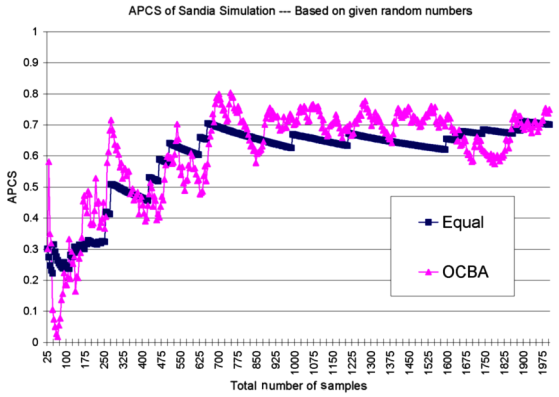

Fig. 14 APCS associated with the identified best design 5.

C. Optimal-Computing-Budget-Allocation (Efficient Ordinal Assurance) Final Phase of the Method

For increased confidence regarding the final optimum, the simultaneous OCBA method can be applied to the final design point and to any alternatives that the user deems to be approximately competitive with it. All of the alternatives that are quasi competitive with the PFS-identified optimum should be included in the OCBA round of sampling, because if another alternative is actually better than the PFS optimum, the OCBA process will identify that alternative. There is relatively little cost penalty for any included alternatives that are not competitive with the actual best alternative; the OCBA algorithm determines this quite early and deemphasizes those designs fairly quickly in its optimized sampling allocation among the various designs. For these reasons, in the final OCBA step of our adaptive OUU method, it is good practice to be somewhat generous with the pool of candidates deemed to be legitimately competitive designs.

For the present demonstration purposes, we include designs 2a, 4a, 6a, 8a, and 5 for the OCBA round of sampling. We start from an initial condition of four samples per design, from the PFS phase of sampling. Figure 13 shows the running number of samples allocated to each design, as a function of the running total number of samples allocated during the OCBA process. The more competitive designs 2a, 4a, and 5, with failure probabilities 0.413, 0.431, and 0.451, respectively, get the most samples. The best design, 5, gets the most samples. The OCBA algorithm devotes most samples to the several best designs as it endeavors to isolate the highest-probability design and maximize the P{CS} probability that it is indeed the best design. Each of these three designs gets more samples than it would if all five designs were sampled equally, as shown by the equal sampling curve in the figure. In stark contrast, the two noncompetitive designs 6a and 8a, with failure probabilities 0.295 and 0.258, respectively, get far less than equal sampling.

Figure 14 shows the associated APCS as a function of the running total number of samples allocated. The calculated APCS value for OCBA sampling is seen to vary wildly in the early sampling and to continue to possess significant stochastic variability or noise at higher numbers of samples. In particular, the APCS value quickly shoots up by ~0.3 from a value of 0.3 to 0.58 in going from 25 to 30 samples. It then promptly declines to as low as 0.02 at 65 samples, before beginning to go back up again in a relatively strong climb to APCS = 0.72 at 275 samples. During this climb, there are a couple of short periods of substantial falloff of APCS, on the order of a 0.2 drop in value. From the local peak of APCS = 0.72, a ~0.3 dropoff in magnitude to 0.39 at 455 samples occurs. From this local minimum, another nonmonotonic climb occurs, to a local maximum of APCS = 0.70 at 535 samples. A subsequent dropoff of about 0.2 occurs, to a local minimum of 0.48 at 625 samples. Then another strong but nonmonotonic climb of about 0.3 in magnitude occurs, to a local peak of APCS = 0.8 at 700 samples. From there, the climbing trend pauses, out through 2000 samples, at which point the sampling was stopped. In this last range, APCS actively varies within an envelope of effective lower and upper bands of 0.6 and 0.8.

We note that the calculated APCS value here applies only to the design alternatives actually included in the APCS evaluation. That is, in the APCS evaluation, we could have also included designs 2, 4, 6, and 8 that were sampled in the PFS phase of the process, just to concretely affirm that these designs too are dominated by design 5 to a level of APCS that would not be much different from the present one. We also observe that Fig. 9 suggests that the maximum failure probability may be slightly to the left of the center point 5. The maximum is evidently within the region of resolution uncertainty about point 5 that is affiliated with the final probing scale of the design space. Hence, we caution that APCS is not the estimated probability that the optimum in the design space was found, but only the probability associated with the identified optimum among the finite number of design points actually evaluated in the design space.

We also note that if we had used a different initial seed for correlated Monte Carlo sampling of all the designs, curves somewhat different from those in Figs. 13 and 14 would have resulted. Yet, the expectation of the random processes would be the same:

1) In the expectation, APCS rises, but at a decreasing rate, as the total number of samples increases.

2) The expected noise level in calculated APCS decreases as the total number of samples increases.

3) The expected noise level in APCS is smaller for equal sampling, but its mean APCS value rises slower than for OCBA sampling.

The noise variation in calculated APCS values seen in this example is not out of the ordinary, except perhaps for the very large dip of 0.56 at 65 samples for OCBA APCS. Although this is uncommon in our other experiences, when the top designs are very close in probabilistic behavior, the variability of calculated APCS is generally relatively large for small numbers of samples. We note that the expectation is for OCBA APCS to converge to 1.0 faster than equal-sampling APCS, but the OCBA APCS estimate also tends to have greater variance.

Finally, we observe that a "knee" in the OCBA APCS curve seems to occur once a value of APCS = 0.7 is first reached. This is also generally true in other applications with which we have experience. It seems that once OCBA APCS first reaches 0.70, there is no need to continue sampling any further, even if very high assurance is desired that the correct design was selected. The other argument here is that the cost of raising APCS beyond 0.6 or 0.7 begins to much more quickly accelerate beyond this point. Hence, we generally recommend OCBA APCS = 0.6 to 0.7 as the cost-effective point at which sampling can be stopped. We note here that OCBA APCS first reaches 0.7 at 275 total samples, whereas equal-sampling APCS takes 655 samples (over 2.38 times as much) to first reach 0.7. For reaching an APCS value of 0.6, OCBA costs 265 samples, whereas equal sampling costs 505 samples (not quite twice as much). Thus, even with the faster-converging OCBA method, it took over an order of magnitude more samples beyond PFS to substantiate with high certainty the correctness of the early indication.

V. Conclusions

Several fundamental concepts of continuous-variable probabilistic ordinal optimization were introduced and demonstrated in this paper. These are 1) ordinal selection or ranking of design alternatives based on statistical figures of merit of the probabilistic behaviors of the candidate designs, 2) the corresponding probability, P{CS}, of correctly selecting the best (or several best) design(s) among the alternatives considered, 3) optimal computing budget allocation for optimally efficient sample allocation for maximizing P{CS} given a fixed number of total samples to be distributed among the alternatives or for minimizing the total number of samples required to attain a stipulated P{CS} level, and 4) tremendous efficiencies to be gained from exploiting spatial correlation of uncertainty in continuous-variable design problems.

Though only very simple and elementary implementations of ordinal-optimization concepts were demonstrated here, promising efficiency versus nonordinal OUU approaches was demonstrated on the two design-variable, two uncertain-variable, probabilistic optimization problem solved here. Much more sophisticated and

efficient implementational possibilities are foreseen. Certainly, there are many areas to be researched in the future involving 1) optimization constraints, 2) advanced ordinal optimizers for searching and progressing in the design space, and 3) increased sampling efficiencies from advanced sampling methods that exhibit significant variance reduction in calculated statistics (therefore faster resolution of P{CS}). For instance, [21] reviews some low-variance sampling methods in the course of introducing some promising new ones. Specialized uncertainty sampling schemes for small-probability values such as importance sampling [22] may also be applicable, as well as sampling schemes for epistemic uncertainties [23]. The many possibilities have only just begun to be identified here.

Ultimately, efficient implementations of probabilistic ordinal optimization may prove to be a reference standard to which the efficiency and accuracy of other OUU approaches can be compared and evaluated. This is analogous to the position that Monte Carlo sampling holds among uncertainty propagation approaches.

Finally, during the refereeing process for this paper, we encountered and answered a reviewer's comment that has important implications that are likely of interest to other readers. We paraphrase the reviewer as saying that an ordinal approach might not be able to solve a typical reliability-based design optimization (RBDO) problem such as minimizing design cost subject to reliability constraints (requirements) on design performance. Although we are not certain that this cannot be done procedurally (earlier, we listed optimization constraints as an area for future research), we believe that treating reliability as a constraint in model-based optimization is not a realistic way to proceed. In view of the magnitudes of model verification and validation-type errors in typical computational physics models, it is concluded in [19] that reliability at small probability levels, say less than 10^{-3}, cannot be reasonably shown (validated) to be accurately estimable with models.

However, a potential *satisficing* approximation to validation can be employed, as discussed in [24]. Nonetheless, it is difficult to see how this subjective inverse "info-gap" procedure might be packaged into an optimization formalism that adequately validates calculated reliability levels in a RBDO problem. Certainly, no such validation procedures seem to exist in the many RBDO frameworks and demonstrations that we have seen in the literature to date.

Nevertheless, it may be that ordinal or ranking accuracy is often sufficient for reliability predictions to be used in a relative sense (as in our application problem) to discriminate which of several neighboring design options has the lowest or highest failure probability. Thus, we believe OUU problems can be realistically posed in terms of maximizing reliability subject to cost constraints, for example, but not in terms of minimizing cost subject to reliability constraints. We thank the reviewer for bringing this issue to the fore, which we originally did not plan to mention in this paper because of our likely controversial stance on it. In the end, because we are aware of much evidence supporting our stance and no empirical evidence against it, we decided to include it in this paper.

Acknowledgments

Supported in part by the National Science Council of the Republic of China under grant NSC 95-2811-E-002-009, by the National Science Foundation under grant IIS-0325074, by NASA Ames Research Center under grants NAG-2-1643 and NNA05CV26G, and by the Federal Aviation Administration under grant 00-G-016. Sandia is a multiprogram laboratory operated by Sandia Corporation, a Lockheed Martin Company, for the U.S. Department of Energy's National Nuclear Security Administration under contract DE-AC04-94AL85000.

References

[1] Ho, Y. C., "An Explanation of Ordinal Optimization: Soft Computing for Hard Problems," *Information Sciences*, Vol. 113, No. 3–4, 1999, pp. 169–192.

[2] Hart, W. E., "Evolutionary Pattern Search Algorithms," Sandia National Labs., Rept. SAND95-2293, Albuquerque, NM, Sept. 1995.

[3] Hough, P. D., Kolda, T. G., and Torczon, V. J., "Asynchronous Parallel Pattern Search for Nonlinear Optimization," *SIAM Journal on Scientific Computing*, Vol. 23, No. 1, 2002, pp. 134–156.

[4] Jones, D. R., Perttunen, C. D., and Stuckman, B. E., "Lipschitzian Optimization Without the Lipschitz Constant," *Journal of Optimization Theory and Applications*, Vol. 79, No. 1, 1993, pp. 157–181.

[5] Spall, J. C., *Introduction to Stochastic Search and Optimization: Estimation, Simulation, and Control*, Wiley, New York, 2003.

[6] Romero, V. J., Eldred, M. S., Bohnhoff, W. J., and Outka, D. E., "Application of Optimization to the Inverse Problem of Finding the Worst-Case Heating Configuration in a Fire," *Numerical Methods in Thermal Problems*, edited by R. W. Lewis, and P. Durbetaki, Vol. 9, Part 2, Pineridge Press, Swansea, England, U.K., 1995, pp. 1022–1033 .

[7] Eldred, M. S., Outka, D. E., Bohnhoff, W. J., Witkowski, W. P., Romero, V. J., Ponslet, E. J., and Chen, K. S., "Optimization of Complex Mechanics Simulations with Object-Oriented Software Design," *Computer Modeling and Simulation in Engineering*, Vol. 1, No. 3, 1996, pp. 323–352.

[8] Eldred, M. S., Hart, W. E., Bohnhoff, W. J., Romero, V. J., Hutchinson, S. A., and Salinger, A. G., "Utilizing Object-Oriented Design to Build Advanced Optimization Strategies with Generic Implementation," *Proceedings of the 6th AIAA/USAF/NASA/ISSMO Symposium on Multidisciplinary Analysis and Optimization*, AIAA, Reston, VA, 1996, pp. 1568–1582; also AIAA Paper 96-4164.

[9] Romero, V. J., "Efficient Global Optimization Under Conditions of Noise and Uncertainty—A Multi-Model Multi-Grid Windowing Approach," *Proceedings of the 3rd WCSMO (World Congress of Structural and Multidisciplinary Optimization) Conference* [CD-ROM], Univ. at Buffalo, State Univ. of New York, Buffalo, NY, 1999.

[10] Alexandrov, N., Dennis, J. E., Jr., Lewis, R. M., and Torczon, V., "A Trust Region Framework for Managing the Use of Approximation Models in Optimization," *Structural Optimization*, Vol. 15, No. 1, 1998, pp. 16–23.

[11] Rodriguez, J. F., Renaud, J. D., and Watson, L. T., "Trust Region Augmented Lagrangian Methods for Sequential Response Surface Approximation and Optimization," ASME Design Engineering Technical Conference, American Society of Mechanical Engineers Paper 97-DETC/DAC-3773, 1997.

[12] Ho, Y. C., Screenivas, R., and Vakili, P., "Ordinal Optimization of Discrete Event Dynamical Systems," *Discrete Event Dynamic Systems: Theory and Applications;Designs, Codes and Cryptography*, Vol. 2, No. 2, 1992, pp. 61–88.

[13] Ba-abbad, M. A., Kapania, R. K., and Nikolaidis, E., "A New Approach for System Reliability-Based Design Optimization," *Reliability and Robust Design in Automotive Engineering 2005*, SP-1956, Society of Automotive Engineers, Warrendale, PA, 2005, pp. 53–64; also Society of Automotive Engineers Paper 2005-01-0348.

[14] Eldred, M. S., Giunta, A. A., Wojtkiewicz, S. F., and Trucano, T. G., "Formulations for Surrogate-Based Optimization Under Uncertainty," 9th AIAA/ISSMO Symposium of Multidisciplinary Analysis and Optimization, Atlanta, GA, AIAA Paper 2002-5585, 2002.

[15] Romero, V. J., "Efficiencies from Spatially Correlated Uncertainty and Sampling in Continuous-Variable Ordinal Optimization," *Journal of Mechanical Design* (submitted for publication).

[16] Romero, V. J., Ayon, D., and Chen, C. H., "Demonstration of Probabilistic Ordinal Optimization Concepts for Continuous-Variable Optimization Under Uncertainty," *Optimization and Engineering*, Vol. 7, No. 3, 2006, pp. 343–365.

[17] Dai, L., "Convergence Properties of Ordinal Comparison in the Simulation of Discrete Event Dynamic Systems," *Journal of Optimization Theory and Applications*, Vol. 91, No. 2, 1996, pp. 363–388.

[18] Chen, C. H., Lin, J., Yucesan, E., and Chick, S. E., "Simulation Budget Allocation for Further Enhancing the Efficiency of Ordinal Optimization," *Discrete Event Dynamic Systems: Theory and Applications;Designs, Codes and Cryptography*, Vol. 10, No. 3, 2000, pp. 251–270.

[19] Romero, V. J., "Characterization, Costing, and Selection of Uncertainty Propagation Methods for Use with Large Computational Physics Models," 42nd Structures, Structural Dynamics, and Materials Conference, Seattle, WA, AIAA Paper 2001-1653, 2001.

[20] Deng, M., Ho, Y. C., and Hu, J. Q., "Effect of Correlated Estimation Errors in Ordinal Optimization," *1992 Winter Simulation Conference*, edited by J. J. Swain, D. Goldsman, R. C. Crain, and J. R. Wilson, ACM Press, New York, 1992, pp. .

[21] Romero, V. J., Burkardt, J. S., Gunzburger, M. D., and Peterson, J. S., "Comparison of Pure and 'Latinized' Centroidal Voronoi Tessellation Against Various Other Statistical Sampling Methods," *Reliability*

Engineering and System Safety, Vol. 91, No. 10–11, 2006, pp. 1266–1280.

[22] Harbitz, A., "Efficient and Accurate Probability of Failure Calculation by Use of the Importance Sampling Technique," *Applications of Statistics and Probability in Soil and Structural Engineering*, edited by G. Augusti, Pitagora, Bologna, Italy, 1983.

[23] Yager, R. R., Fedrizzi, M., and Kacprzyk, J. (eds.), *Advances in the Dempster-Shafer Theory of Evidence*, Wiley, New York, 1994.

[24] Romero, V., "Some Issues in Quantification of Margins and Uncertainty (QMU) for Phenomenologically Complex Coupled Systems," 8th AIAA Non-Deterministic Approaches Conference, Newport, RI, AIAA Paper 2006-1989, 2006.

N. Alexandrov
Associate Editor